THE ANATOLIAN JOURNAL OF CARDIOLOGY

Official journal of the TURKISH SOCIETY OF CARDIOLOGY

Hsa-circ-ACSL1 Enhances Apoptosis and Autophagy in Myocarditis Cardiomyocytes Through the miR-7-5p/XBP1 Axis

ORIGINAL INVESTIGATION

ABSTRACT

Background: Viral myocarditis (VMC) is a common cardiovascular disease, and circular RNAs (circRNAs) have been identified to play an important role in the pathophysiology of cardiovascular disease. However, the clinical signifi ance, biological functions, and regulatory mechanisms of circRNAs in VMC remain poorly understood. Therefore, this study explored the biological functions and regulatory mechanisms of circ-ACSL1 in VMC.

Methods: The animal and cell models of VMC were established by infecting BABL/C mice and interleukin-2 cells with coxsackievirus B3 (CVB3). Pro-inflamma ory factors, markers of myocardial injury, apoptosis, and autophagy were detected to evaluate the degree of myocardial inflammation and myocardial injury after altering circ-ACSL1, microRNA-7-5p (miR-7-5p), and X-box binding protein 1 (XBP1) expression alone or in combination.

Results: Knocking down circ-ACSL1 could inhibit inflammation, autophagy, and apoptosis in VMC animals and cells. Mechanistically, circ-ACSL1 targeted miR-7-5p to regulate the downstream target XBP1. In addition, depleting miR-7-5p rescued the therapeutic effect of depleting circ-ACSL1. Overexpression of circ-ACSL1 aggravated VMC; however, this effect was saved by knocking down XBP1.

Conclusion: By competitively absorbing miR-7-5p, circ-ACSL1 increases XBP1 expression and aggravates myocardial inflammation. Meaningfully, VMC treatment may benefit from circ-ACSL1 as a potential biomarker for precise diagnosis and as a potential therapeutic target.

Keywords: Hsa_circ_ACSL1, miR-7-5p, viral myocarditis, XBP1

INTRODUCTION

Myocarditis (MC) is an inflamma ory disease that involves the myocardium and leads to cardiomyopathy. It is caused by a variety of causes such as immune damage, bacterial infection, viral infection, etc.,[1] and is a potentially life-threatening myocardial inflamma ory disease.[2] Viral infection is the most common type of MC, and coxsackievirus B3 (CVB3), a cardiac virus, is the most common cause of MC.[3] In some cases, viral MC (VMC) can progress to chronic MC, dilated cardiomyopathy, and congestive heart failure, which may require a heart transplant.[4]

The autophagic process involves the degradation and recycling of unwanted proteins, organelles, and other cellular components.[5] The process of autophagy is generally seen as a protective response to stress.[6] Viruses can utilize autophagy to evade degradation and facilitate viral replication and acquisition of metabolites, while over-activated autophagy also promotes apoptosis and inflamma ory cascades.[7] In the body, apoptosis occurs naturally, regulating cell death as part of homeostasis. As cell survival is determined by the balance between autophagy and apoptosis, autophagy has a complex relationship with apoptosis.[8]

The discovery and exploration of circular RNAs (circRNAs) date back decades.[9] It has been reported that circRNAs are involved in many pathophysiological processes due to various biological functions.[10] In addition, circRNA is generally low in expression and often exhibit cell type and tissue specificit .[11] circ-ACSL1 shows up-regulated expression in MC and has pro-inflamma ory properties in MC.[12]

Fu Li Liang[#]
You Fu Tong[#]
Xiao Chun Zhang
Xiao Feng Ma

Department of Coronary Heart Disease II, Qinghai Cardio-Cerebrovascular Specialty Hospital, Qinghai High Altitude Medical Research Institute, Xining City, Qinghai Province, China

Corresponding author:
Xiao Feng Ma
maxiaofengmua@hotmail.com

Received: March 28, 2024
Accepted: July 2, 2024
Available Online Date: October 7, 2024

Cite this article as: Liang FL, Tong YF, Zhang XC, Ma XF. Hsa-circ-ACSL1 enhances apoptosis and autophagy in myocarditis cardiomyocytes through the miR-7-5p/XBP1 axis. *Anatol J Cardiol.* 2024;28(11):523-532.

[#]These authors contributed equally to this work.

DOI:10.14744/AnatolJCardiol.2024.4472

Moreover, hsa-circ-ACSL1 may constitute as a potential biomarker for fulminant MC.[13] However, circ-ACSL1 is not well-explored from a biological perspective in MC. In terms of mechanism, emerging reports support that circRNA can act as a competing endogenous RNA to regulate messenger RNA (mRNA) expression via spongy micro RNAs (miRNAs).[14-17]

miR-7-5p, a type of microRNA, has been shown to be regulated by circRNAs.[18] microRNA-7 is reported to be upregulated in ischemia/reperfusion (I/R) injury.[19,20] However, miR-7-5p shows low expression after I/R injury. Nevertheless, there are no studies reported on the expression of miR-7-5p in VMC. XBP1, as a key regulator of endoplasmic reticulum stress (ERS) and phase unfolded protein response signaling pathways, plays a critical role in regulating cellular autophagy and apoptosis due to ERS.[21] Inactivation of XBP1 splicing leads to cellular death after chronic or irreversible sensitivity to cell death due to ERS. X-box binding protein 1 (XBP1) is a signaling pathway protein involved in inflamma ory signaling cascades, and several studies have demonstrated that it plays an important regulatory role in MC.[22] However, the specific regulatory mechanism between circACSL1, miR-7-5p, and XBP1 remains unclear.

Based on this, the present study intends to investigate the mechanism of action of circ-ACSL1 involved in the pathogenesis and progression of VMC and promotion of apoptosis and autophagy in MC cardiomyocytes through circRNA–miRNA–mRNA network. Elucidation of the potential molecular mechanisms mediated by circACSL1 may lead to the development of promising therapeutic candidates for VMC.

METHODS

Laboratory Animals and Viruses

Thirty male BABL/C mice (4-6 weeks, 16-19 g) were purchased from SLAC Laboratory Animal Co., Ltd. (Shanghai, China). A standard diet and water were provided to the mice for a week, and they were kept at 25 ± 2°C with 60-70% humidity and a 12-hour light/dark cycle.

CVB3 was obtained (ATCC, USA), and HL-1 cells (ATCC) were used as vectors for CVB3 replication. The virus titer of CVB3 was determined using the tissue culture infectious dose 50 (TCID50) method.

VMC Animal Model

BABL/C mice were randomly divided into normal group, CVB3 group, sh-ACSL1 group, and sh-NC group (6 mice per group). In the normal group, 100 µL phosphate buffered saline (PBS) was injected intraperitoneally, while 100 µL CVB3 diluted in PBS (10^3 TCID50) was injected intraperitoneally in the other 3 groups. Body weight and death were recorded daily. Seven days after injection, blood samples were collected from the eyeball, and serum was separated by centrifugation at 3000 × *g* for 10 minutes and stored at −80°C. The mice were then euthanized by inhaling excess CO_2, and hearts were taken and dried with saline (2°C). The lower one-third of the heart was fi ed in 10% paraformaldehyde for tissue sections and the remaining portions were stored at −80℃.

Lentivirus Injection

The mice were injected with 100 µL of circ-ACSL1 shRNA lentiviral vector (sh-ACSL1) or sh-NC (1×10^8 TU/mL) through the tail vein on days 3 and 5 after CVB3 infection. The lentiviral vectors were synthesized by GenePharma (Shanghai, China).

Terminal Deoxynucleotidyl Transferase dUTP Nick-End Labeling (TUNEL) Staining

Myocardial tissues fi ed in 10% paraformaldehyde were sectioned to 4 µm after paraffin embedding. Tissue paraffin sections were washed with xylene for 5 minutes and treated with 100%, 95%, 90%, 80%, and 70% ethanol, each for 3 minutes. The myocardial tissues were then treated with protease K for 30 minutes, soaked in a blocking buffer for 10 minutes, and added with a mixture of TdT (2 µL) and green fluo escent fluo escein isothiocyanate (FITC) probe-labeled dUTP (48 µL) (Beyotime, Shanghai, China) for 1 hour. The tissues were sealed with an anti-fluo escence quencher and observed under a fluo escence microscope. Nuclei were stained with DAPI. TUNEL positive cells (%) = number of green cells/total cells × 100%.

Enzyme-Linked Immunosorbent Assay (ELISA)

Creatine Kinase Isoenzymes (CK-MB), Cardiac troponin I (cTnI), and B-type natriuretic peptide (BNP) in serum and cells were measured by Mouse CK-MB ELISA Kit, Mouse TNNI3/cTn-I ELISA Kit, and BNP ELISA Kit, respectively. Interleukin-6 (IL-6), interleukin-1β (IL-β), and tumor necrosis factor-α (TNF-α) in myocardial tissue and cell culture supernatant were determined by ELISA Kits. All the above kits were purchased from Sangon (Shanghai, China). Optical density was measured using a microplate reader (EL 340, Bio-Tek Instruments, USA).

Western Blot

Myocardial tissue and cells were separately lysed in radioimmunoprecipitation lysis buffer (Beyotime). Proteins that were extracted were quantified by a bicinchoninic acid kit (Beyotime). Proteins were mixed with a sample buffer (Beyotime) and treated in a boiling water bath for 3 minutes. After electrophoresis at 80 V for 30 minutes, the separation continued at 120 V for 1-2 hours. The proteins were transferred to a membrane using a 300 mA ice bath for 60 minutes and soaked in a blocking buffer for 60 minutes at room temperature or overnight at 4°C. The protein was combined with anti-β-actin (ab8227, 1 : 1000), LC3B (ab51520, 1 : 3000), Beclin-1 (ab210498, 1 : 1000), Bcl-2 (ab182858, 1 : 2000), Bax (ab182733, 1 : 2000), Cleaved caspase 3 (ab2302, 1 : 500), XBP1 (ab37152, 1 µg/mL), p-p65 (ab86299, 1 : 2000), and p65 (ab16502, 1 : 1000, all from Abcam, UK), and transferred to the secondary antibody (Goat Anti-Rabbit immunoglobulin G, ab205718, 1 : 2000). A developer was added to the

HIGHLIGHTS

- Knocking down circ-ACSL1 inhibits inflammation, apoptosis, and autophagy of VMC cardiomyocytes.
- miR-7-5p downregulation can reduce the therapeutic effect of depleting circ-ACSL1 on VMC.
- circ-ACSL1 overexpression promotes VMC, but this effect is saved by depleting XBP1.

membrane, and protein bands were detected using a chemiluminescent imaging system (Gel Doc XR, Bio-rad).

Cell Culture

HL-1 cells were placed in Dulbecco's modified Eagle medium (Invitrogen) supplemented with 10% fetal bovine serum (Gibco, USA) and 1% penicillin–streptomycin (HyClone, USA) at 37°C with 5% CO_2.

HL-1 cells and CVB3 (100 TCID50) were incubated in a serum-free medium for 2 hours, followed by incubation in a normal medium.

Cell Transfection

circ-ACSL1 and XBP1 were overexpressed using pcDNA3.1 (Invitrogen, Thermo Fisher Scientific). Small interfering RNAs targeting circ-ACSL1 and XBP1 (si-circ-ACSL1 and si-XBP1), as well as negative control siRNAs (si-circ-ACSL1-NC, si-XBP1-NC), miR-7-5p-mimic, miR-7-5p-inhibitor, mimic-NC, and inhibitor-NC, were synthesized by GenePharma. Using Lipofectamine 3000 (Invitrogen), these oligonucleotides and plasmids were transfected into HL-1 cells, and the culture medium was replaced 6 hours later. After 48 hours, transfection efficiency was evaluated using real-time reverse transcriptase-polymerase chain reaction (RT-qPCR) or Western blot.

Flow Cytometry

Apoptotic cells were measured using the FITC annexin V apoptosis assay kit I (BD Biosciences, USA). A cell suspension (3 mL, 1 × 10^5/mL) was centrifuged at 500 r/min for 5 minutes, and the culture medium was discarded after centrifugation. The remaining pellet was centrifuged at 500 r/min for 5 minutes, and the resulting cells were resuspended in 100 µL binding buffer with 5 µL annexin V-FITC and 5 µL propidium iodide (PI). After 15 minutes, FITC and PI fluo escence were detected by fl w cytometry.

Monodansylcadaverine Staining

Autophagy was observed around the positive nuclei, and all acidic vacuoles were stained. Cell slides were prepared overnight and incubated with 0.05 mmol/L monodansylcadaverine (MDC) (Huzheng, Shanghai, China) in a water bath at 37℃ for 15 minutes. After fi ation with 4% paraformaldehyde for 15 minutes, anti-fluo escence quenched slides were observed by fluo escence microscopy in the dark.

RNAse R Test

Total RNA isolation of HL-1 cells was performed with TRIzol reagent (Invitrogen). Then, 2 µg RNA was incubated with 5 U/µg RNAse R (Epicentre Technologies, USA) at 37℃ for 24 hours. Linear RNA and circular RNA were analyzed by RT-qPCR.

Actinomycetes D Test

A total RNA sample was extracted from HL-1 cells after exposure to 100 ng/mL actinomycin D (Merck, Germany) at 0, 4, 8, 12, and 24 hours for RT-qPCR analysis of circ-ACSL1 stability.

Reverse Transcriptase-Polymerase Chain Reaction

Total RNA was extracted from cardiomyocytes and tissues using SparkZol reagent (SparkJade, China). The quantity and quality of total RNA were estimated with a NanoDrop ND-2000 spectrophotometer (NanoDrop, USA). Complementary DNA (cDNA) was synthesized using Evo M-MLV RT Premix (AG 11706, ACCURATE BIOTECHNOLOGY, China) and Mir-XTM miRNA fir t chain synthesis Kit (Takara, Dalian, China). RT-qPCR was performed with the SYBR Green Premix Pro Taq HS qPCR Kit (AG 11701, ACCURATE BIOTECHNOLOGY). Primers are shown in Table 1. RNA expression was quantified on the LightCycler 480 system (Roche Diagnostics, Switzerland), and miR-7-5p was normalized with respect to U6 expression, and other RNAs were normalized with respect to β-actin. Quantifi ation results were determined by $2^{-\Delta\Delta CT}$ method.

RNA Pull Down

Using the TranscriptAid T7 high-yield transcription Kit (Thermo Fisher Scientific), miR-7-5p wild type (WT) and mutant (Mut) miR-7-5p were transcribed. Biotinized miR-7-5p-WT or miR-7-5p-Mut were incubated with cell lysate at 48°C for 1 hour. After purifi ation, RNA was eluted with elution buffer, and RT-qPCR was performed to check circ-ACSL1 and XBP1 expression.

Luciferase Reporter Gene Assay

Potential binding sequences of miR-7-5p to circ-ACSL1 and XBP1 3′-UTR were predicted by starBase database (http://starbase.sysu.edu.cn/). Mutations were then constructed into the potential binding sequences using site-specific mutagenesis kits (Stratagene, USA). The constructed binding sequences of circ-ACSL1 and XBP1 were subcloned into the pmirGLO vector (Promega, USA) and transfected with miR-7-5p mimic or mimic NC into HL-1 cells using Lipofectamine 2000. After 48 hours, luciferase activity was detected in the dual luciferase reporter assay system (Promega).

Table 1. Sequences of Primers in PCR

Gene	Forward	Reverse
mmu-circ-ACSL1	AACCACCAACCCAGAACCAT	ACTGCCGAATGTCAATCAGC
miR-7-5p	ACACTCCAGCTGGGTGGAAGACTAGTGATTTT	ACACTCCAGCTGGGTGGAAGACTAGTGATTTT
mmu-ACSL1	GACGACCTCAAGGTGCTTCA	ACCCAGGCTCGACTGTATCT
mmu-XBP1	AAACAGAGTAGCAGCACAGACTGC	TCCTTCTGGGTAGACCTCTGGGAG
mmu-β-actin	CATCCGTAAAGACCTCTATGCCAAC	ATGGAGCCACCGATCCACA
mmu-U6	CTCGCTTCGGCAGCACA	AACGCTTCACGAATTTGCGT

circ-ACSL1, circular RNA ACSL1; miR-7-5p, microRNA-7-5p; XBP1, X-box binding protein 1

Statistical Analysis

Statistical analysis was carried out using SPSS v.24.0 software, and visualization of data was obtained by Graphpad prism 8.0 software. Results were obtained from at least 3 independent replicated experiments. The normality of data distribution was assessed in this study using the Shapiro–Wilk test, and data were expressed as mean ± SD. The 2-tailed Student's *t*-test was used for comparison between 2 groups, and 1-way ANOVA was used for comparison between multiple groups. *P*-value < .05 was considered to indicate statistically signifi ant. No artificial intelligence-assisted technologies were used in the production of this manuscript.

RESULTS

High Expression and Stability of Circ-ACSL1 in VMC

The volcano map of differential expression and function of circRNAs in children with fulminant MC[13] showed that circ-ACSL1 was up-regulated (Figure 1A). Hierarchical cluster analysis showed that circRNA expression levels could be distinguished in the relevant heat maps (Figure 1B).

After CVB3 injection, mice injected with CVB3 continued to lose weight from day 3 (Figure 1C). ELISA results indicated that IL-1β, IL-6, and TNF-α were increased in mouse myocardial tissue and infected HL-1 cells (Figure 1D and E), and the upward trend was detected in myocardial injury markers CK-MB, cTnI, and BNP (Figure 1F and G). Flow cytometry found that the apoptosis rate of HL-1 cells infected with CVB3 was elevated (Figure 1H). Western blot analysis of apoptotic proteins indicated that cleaved-caspase-3 and Bax in myocardial tissue and HL-1 cells infected with CVB3 were increased. However, Bcl-2 protein was decreased (Figure 1I and J). Monodansylcadaverine staining showed that the number of autophagosomes in HL-1 cells was increased after CVB3 infection (Figure 1K). TUNEL staining showed that the apoptosis rate in myocardial tissue in mice infected with CVB3 was increased (Figure 1L). Moreover, Western blot detected that LC3 Ⅱ/LC3 Ⅰ ratio increased in mouse myocardial tissue and HL-1 cells after CVB3 infection, and Beclin-1 was up-regulated (Figure 1M and N). The above data confirmed the successful establishment of VMC animal model and in vitro cell model. circ-ACSL1 was increased in myocardial tissue and HL-1 cells infected with CVB3 by RT-qPCR (Figure 1O).

After RNAse R digestion and actinomycin D treatment, circACSLI in HL-1 cells was detected by RT-qPCR to verify the closed-loop and stability of circACSLI. circ-ACSL1 was resistant to RNAse compared to ACSL1, suggesting that circ-ACSL1 is a circRNA (Figure 1P). The half-life of circ-ACSL1 was more than 24 hours, while that of ACSL1 was about 4 hours, indicating that circ-ACSL1 was more stable than linear ACSL1 (Figure 1Q). The above results suggest that circACSL1 exists as a highly expressed and stable marker in VMC.

Knocking Down circ-ACSL1 Inhibits Inflammation, Apoptosis, and Autophagy of VMC Cardiomyocytes

shRNA lentiviral vectors targeting circ-ACSL1 were injected into VMC mice. The interference RNA si-circ-ACSL1 was transfected into infected HL-1 cells. Then, RT-qPCR confirmed that circ-ACSL1 expression in myocardial tissue and HL-1 cells decreased with the depleting circ-ACSL1 (Figure 2A and B). ELISA analysis showed that IL-1β, IL-6, and TNF-α levels in myocardial tissue and cell supernatant were reduced after circ-ACSL1 knockdown (Figure 2C and D), and CK-MB, cTnI, and BNP in myocardial tissue and HL-1 cells were also decreased after circ-ACSL1 knockdown (Figure 2E and F). TUNEL staining showed that apoptosis in myocardial tissue was alleviated after circ-ACSL1 knockdown (Figure 2G). HL-1 cells were shown to be less susceptible to apoptosis after circ-ACSL1 knockdown by fl w cytometry (Figure 2H). Western blot detected that circ-ACSL1 knockdown decreased caspase-3, cleaved caspase-3, and Bax, and enhanced Bcl-2 protein expression (Figure 2I and J). Monodansylcadaverine staining showed a decrease in autophagosomes in HL-1 cells after circ-ACSL1 knockdown (Figure 2K). Western blot results showed that circ-ACSL1 knockdown decreased LC3 Ⅱ/LC3 Ⅰ ratio and Beclin-1 protein level in mouse myocardial tissue and HL-1 cells (Figure 2L and M). In summary, knockdown of circACSL1 inhibited inflammation, apoptosis, and autophagy in VMC cardiomyocytes.

Circ-ACSL1 Targets miR-7-5p Adsorption

RT-qPCR detected low expression of miR-7-5p in myocardial tissue of VMC mice and CVB3-treated HL-1 cells (Figure 3A). Figure 3B shows the binding sites of circ-ACSL1 to miR-7-5p predicted by StarBase. Dual luciferase reporter experiments showed that miR-7-5p mimic could reduce the luciferase activity of WT-circ-ACSL1, but could not reduce that of Mut-circ-ACSL1 (Figure 3C). To verify whether circ-ACSL1 can interact with miR-7-5p, RNA pull-down experiments were performed in HL-1 cells. The results indicated that the Bio-miR-7-5p-WT group was more enriched in circ-ACSL1 than the Bio-miR-7-5p-Mut group (Figure 3D). RT-qPCR further detected that circ-ACSL1 knockdown increased miR-7-5p in CVB3-infected mice myocardial tissue and HL-1 cells (Figure 3E). Taken together, these results suggest that miR-7-5p can bind to the corresponding site on the circACSL1 transcript, and circACSL1 can target adsorption of miR-7-5p.

miR-7-5p Downregulation can Reduce the Therapeutic Effect of Depleting Circ-ACSL1 on VMC

HL-1 cells were transfected with si-circ-ACSL1 + miR-7-5p inhibitor. RT-qPCR results showed that si-circ-ACSL1 decreased circ-ACSL1 and increased miR-7-5p levels, while the miR-7-5p inhibitor saved the expression increase of miR-7-5p (Figure 4A). Based on circ-ACSL1 knockdown, downregulating miR-7-5p restored IL-1β, IL-6, and TNF-α levels (Figure 4B) as well as cTnT, CK-MB, and BNP contents (Figure 4C). Flow cytometry analysis showed that depleting circ-ACSL1 inhibited apoptosis rate, but this effect was saved after depleting miR-7-5p (Figure 4D). Western blot results demonstrated that circ-ACSL1 knockdown reduced cleaved caspase-3 and Bax and increased Bcl-2 proteins, but this effect was impaired by miR-7-5p knockdown (Figure 4E). Also, LC3 Ⅱ/LC3 Ⅰ ratio of HL-1 cells was decreased after circ-ACSL1 knockout, and Beclin-1 protein was down-regulated. However, this result was saved by depleting miR-7-5p (Figure 4F). Monodansylcadaverine staining of HL-1 cells showed that silencing circ-ACSL1 reduced autophagy, but continued depleting miR-7-5p mitigated this phenomenon

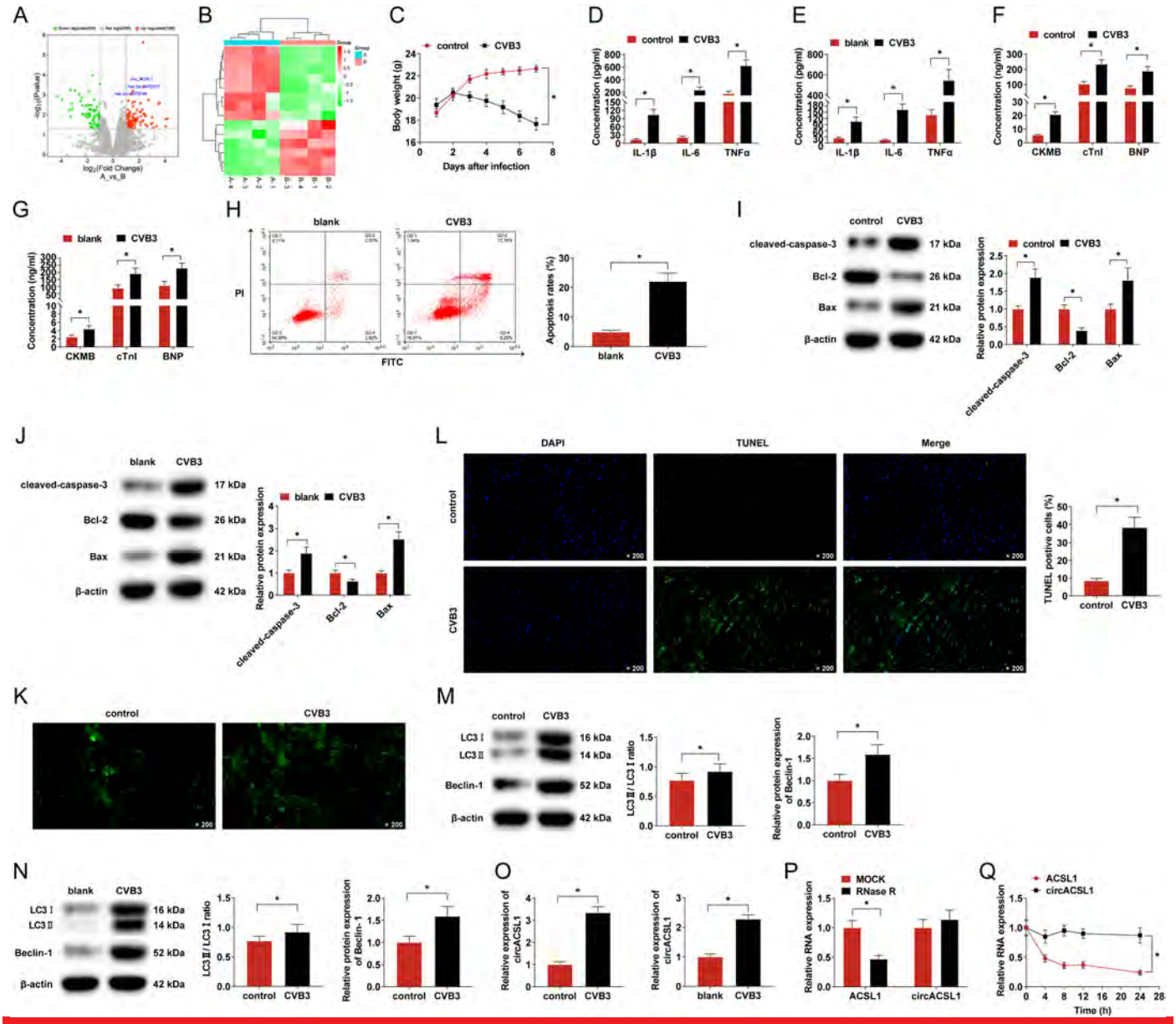

Figure 1. High expression and stability of circ-ACSL1 in VMC. (A) Volcano maps showing differentially expressed circRNAs; (B) hierarchical cluster analysis of circRNAs; (C) weight change of mice; (D and E) ELISA determination of IL-1β, IL-6, and TNF-α in myocardial tissue and HL-1; (F and G) ELISA determination of CK-MB, cTnI, and BNP in mouse serum and HL-1 cell supernatant; (H) fl w cytometry detection of apoptotic rate of HL-1 cells; (I and J) Western blot analysis of caspase-3, cleaved caspase-3, Bcl-2, and Bax in mouse myocardial tissue and HL-1 cells; (K) MDC staining detection of autophagosomes; (L) TUNEL staining of myocardial tissue in mice; (M and N) Western blot analysis of LC3 Ⅱ/LC3 Ⅰ and Beclin-1 in myocardial tissue and HL-1 cells; (O) RT-qPCR detection of circ-ACSL1 expression in mice and HL-1 cells; and (P and Q) analysis of stability of circ-ACSL1. Detailed data in Supplementary Table 1. *$P < .05$.

(Figure 4G). The above results suggest that knockdown of miR-7-5p reverses the therapeutic effect of knockdown of circACSL1.

miR-7-5p Targets XBP1

High expression of XBP1 was detected by RT-qPCR and Western bot in VMC mice and CVB3-treated HL-1 cells (Figure 5A and B). Figure 5C used StarBase to predict the binding site of XBP1 to miR-7-5p. Dual luciferase report experiments showed that miR-7-5p mimic could only reduce the luciferase activity of WT-XBP1 (Figure 5D). RNA Pull-down experiment revealed the enrichment of XBP1 by Bio-miR-7-5p-WT (Figure 5E). RT-qPCR and Western blot further reported that depleting miR-7-5p increased XBP1 expressions in CVB3-infected HL-1 cells (Figure 5F and G). The above results support the ability of miR-7-5p to target and regulate XBP1.

Circ-ACSL1 Overexpression Promotes VMC, But This Effect is Saved by Depleting XBP1

HL-1 cells were transfected with pcDNA-circ-ACSL1, pcDNA-circ-ACSL1 + si-XBP1, and pcDNA, respectively.

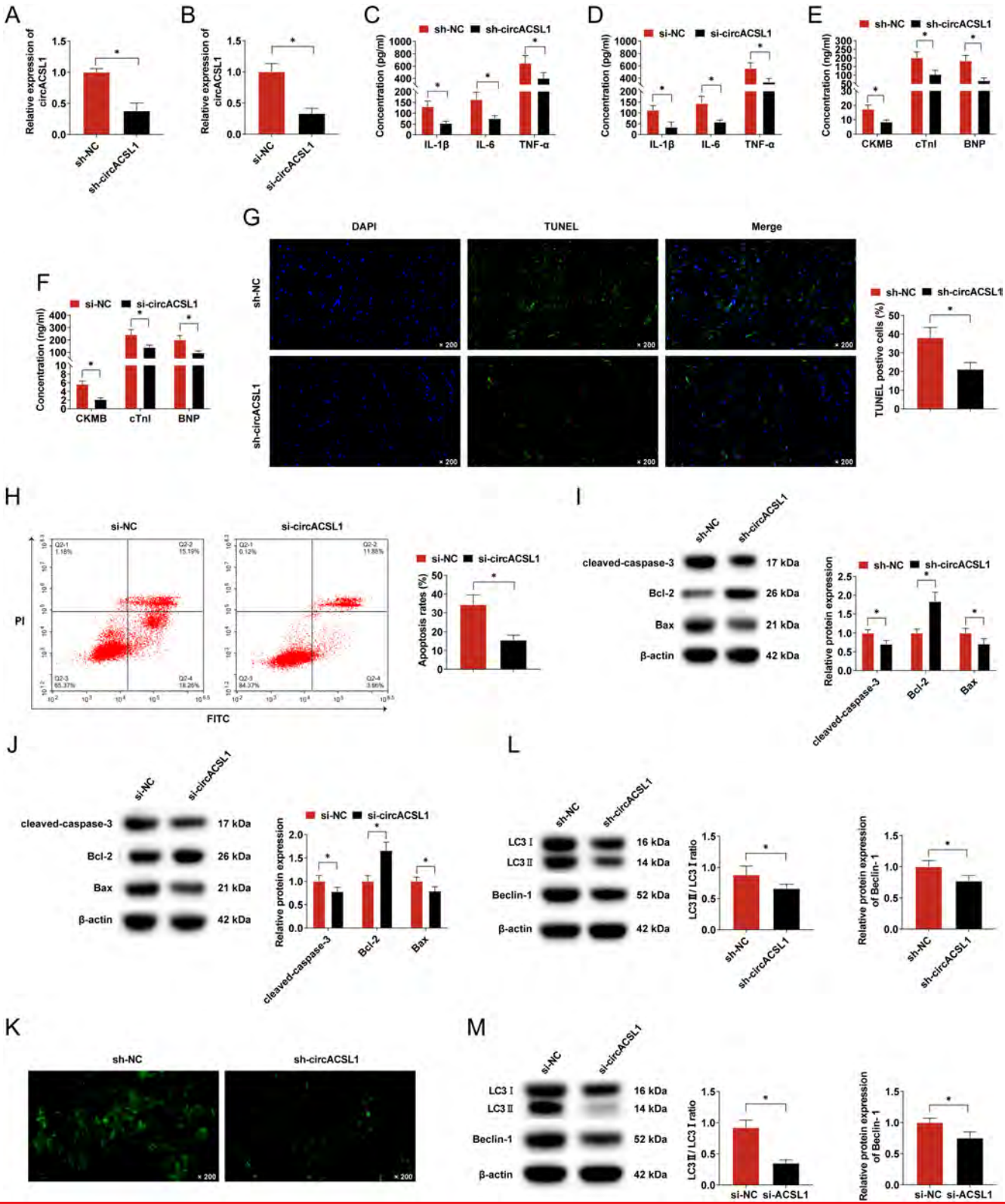

Figure 2. circ-ACSL1 knockdown inhibits inflammation, apoptosis, and autophagy of VMC cardiomyocytes. (A) RT-qPCR detection of circ-ACSL1 in myocardial tissue after circ-ACSL1 knockdown; (B) RT-qPCR detection of circ-ACSL1 in HL-1 after circ-ACSL1 knockdown; (C and D) ELISA determination of IL-1β, IL-6 and TNF-α in myocardial tissue and HL-1 cells; (E and F) ELISA determination of CK-MB, cTnI and BNP in mouse myocardial tissue and HL-1 cell supernatant; (G) TUNEL staining of myocardial tissue; (H) fl w cytometry detection of apoptotic rate of HL-1 cells; (I and J) Western blot analysis of apoptotic proteins in HL-1 cells; (K) MDC staining detection of autophagosomes; (L and M) Western blot analysis of LC3 Ⅱ/LC3 Ⅰ and Beclin-1 in myocardial tissue and HL-1 cells. Detailed data in Supplementary Table 2. *P < .05.

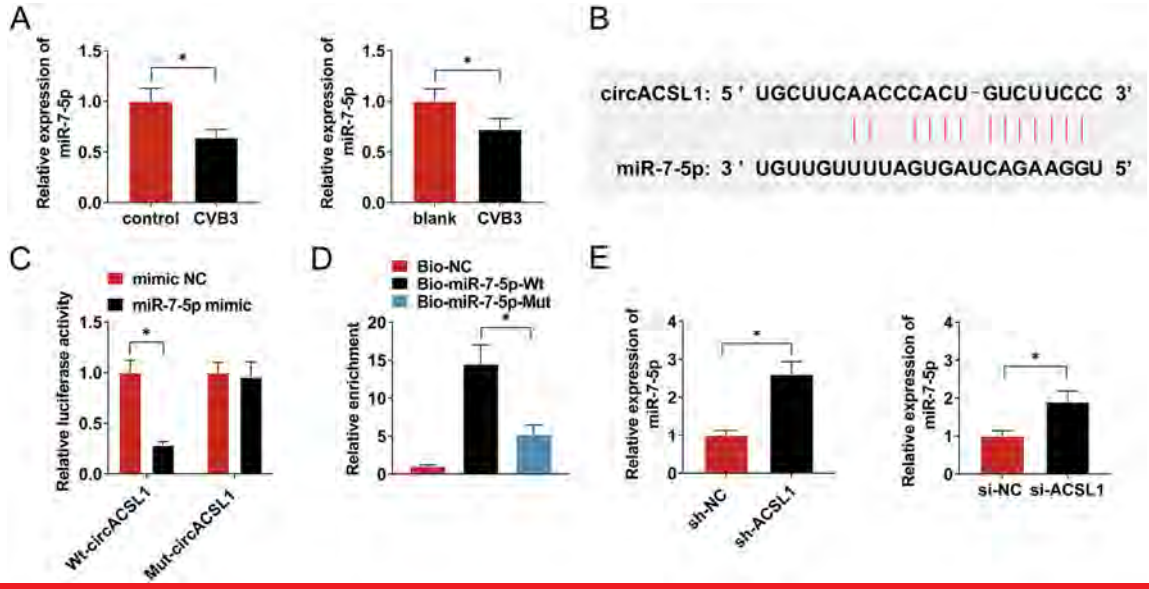

Figure 3. circ-ACSL1 targets miR-7-5p. (A) RT-qPCR detection of miR-7-5p in myocardial tissue and HL-1 cells infected with CVB3; (B) starBase predicted the binding site of miR-7-5p and circ-ACSL1; (C and D) Dual-luciferase reporter gene assay and RNA Pull-down experiment verified the binding of miR-7-5p and circ-ACSL1; (E) RT-qPCR detection of miR-7-5p in mouse myocardial tissue and HL-1 cells. Detailed data in Supplementary Table 3. *P < .05.

RT-qPCR results confirmed that pcDNA-circ-ACSL1 in HL-1 cells enhanced circ-ACSL1 and XBP1 expression, while si-XBP1 saved XBP1 expression (Figure 6A). IL-1β, IL-6, and TNF-α increased after circ-ACSL1 overexpression in HL-1 cells, but this effect was attenuated by knocking down XBP1 (Figure 6B). cTnT, CK-MB, and BNP were increased after

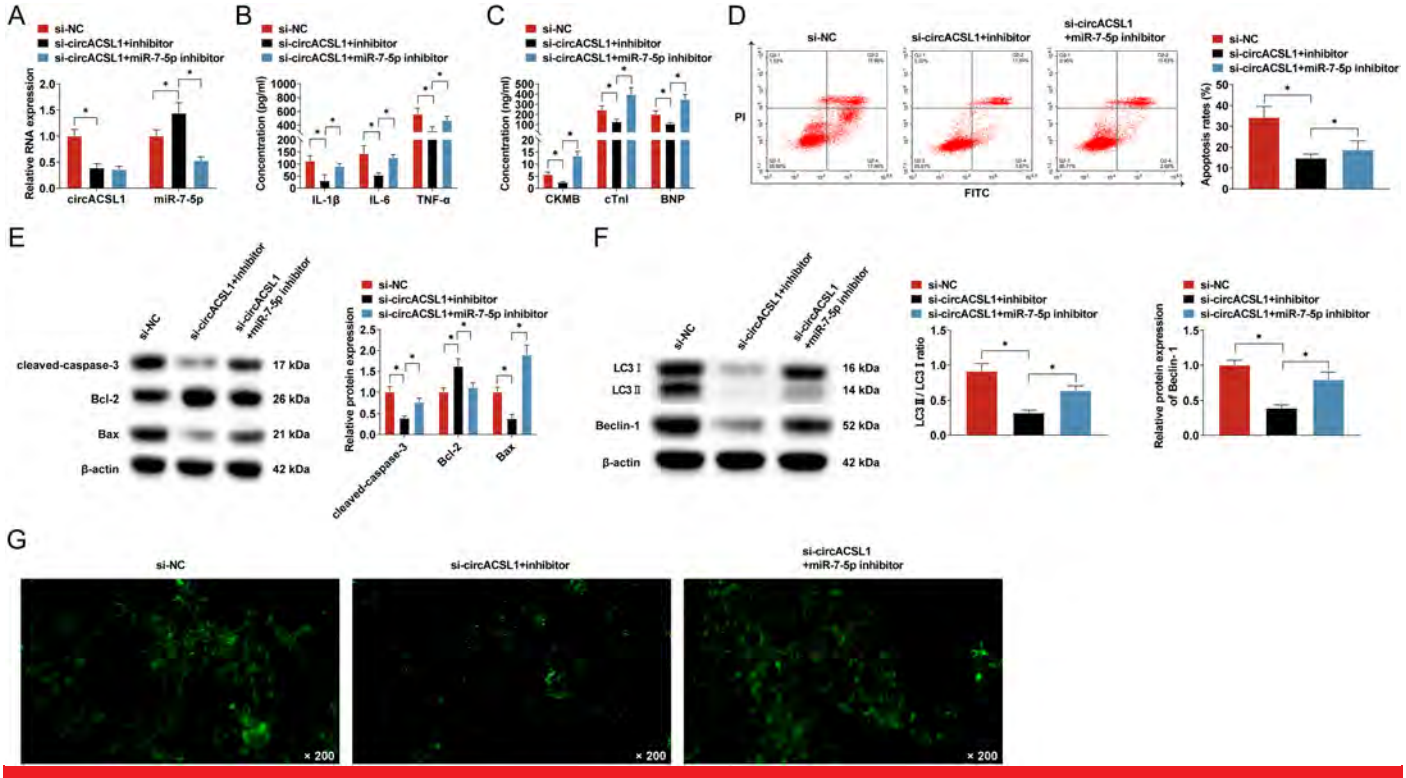

Figure 4. Depleting miR-7-5p can save the therapeutic effect of depleting circ-ACSL1 on VMC. (A) RT-qPCR detection of circ-ACSL1 and miR-7-5p in HL-1 cells; (B) ELISA determination of IL-1β, IL-6 and TNF-α in HL-1 cells; (C) ELISA determination of CK-MB, cTnI, and BNP in HL-1 cell supernatant; (D) fl w cytometry detection of apoptotic rate of HL-1 cells; (E and F) Western blot analysis of apoptotic proteins in HL-1 cells; (G) MDC staining detection of autophagosomes. Detailed data in Supplementary Table 4. *P < .05.

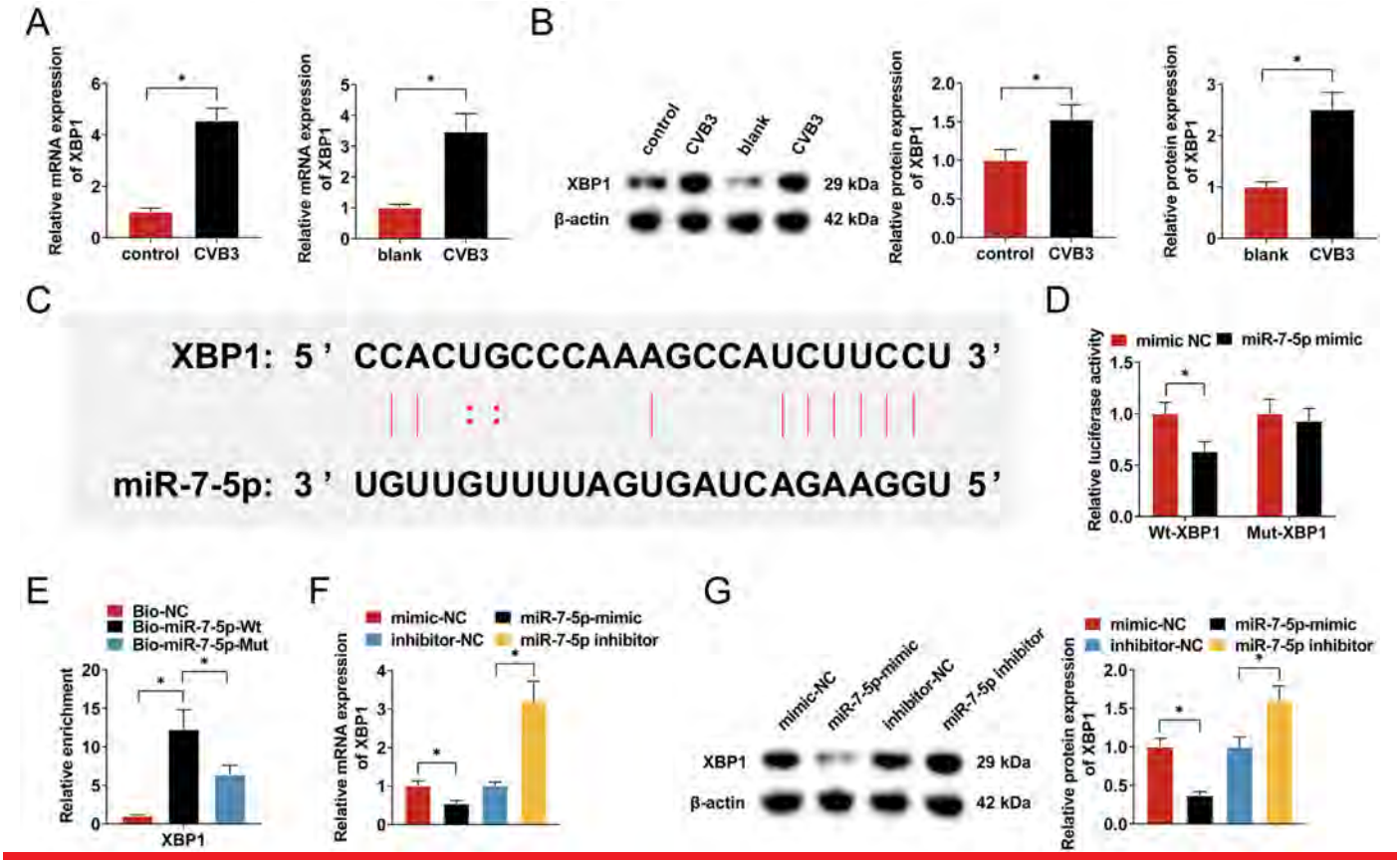

Figure 5. miR-7-5p mediates XBP1 expression. (A and B) RT-qPCR and Western blot detection of XBP1 in myocardial tissue and HL-1 cells infected with CVB3; (C) starBase predicted the binding site of miR-7-5p and XBP1; (D and E) Dual-luciferase reporter gene assay and RNA Pull-down experiment verified the binding of miR-7-5p and XBP1; (F and G) RT-qPCR and Western blot detection of XBP1 in HL-1 cells. Detailed data in Supplementary Table 5. *$P < .05$.

circ-ACSL1 overexpression in HL-1 cells, but this effect was blocked by depleting XBP1 (Figure 6C). Overexpressing circ-ACSL1 could promote apoptosis, but this promoting effect was canceled after depleting XBP1 (Figure 6D). In addition, upregulating circ-ACSL1 increased cleaved-caspase-3 and Bax while it decreased Bcl-2 protein. This effect was partially suppressed by knocking down XBP1 (Figure 6E). LC3 Ⅱ/LC3 Ⅰ ratio of HL-1 cells was increased after overexpression of circ-ACSL1, and Beclin-1 protein was enhanced. These results were mitigated by knocking down XBP1 (Figure 6F). Overexpression of circ-ACSL1 increased autophagosomes, but continued depleting XBP1 saved this phenomenon (Figure 6G). p-p65 protein in XBP1-related inflamma ory pathway was decreased in HL-1 cells, indicating that XBP1 may inhibit the proinflamma ory effect of circ-ACSL1 through certain signaling pathway (Figure 6H). All of the above results suggest that overexpression of circACSL1 promotes myocarditis, but this effect was reversed after knockdown of XBP1.

DISCUSSION

Viral myocarditis (VMC) is an inflamma ory disease resulting from a viral infection, causing immunological responses resulting in dysfunction and impaired contractility in the heart.[23] The molecular regulation of VMC progression remains an elusive problem. There has been a growing body of evidence that circRNAs are crucial regulators of cardiovascular diseases.[24,25] Interference with circRNA HIPK3 alleviates cardiac dysfunction and apoptosis in H9C2 cardiomyocytes in a lipopolysaccharide (LPS)-induced mouse model.[26] In this study, based on a previous study,[13] we analyzed and obtained circRNA expression profiles showing hsa-circ-ACSL1, which showed up-regulated expression in VMC based on volcano and heatmap data. Circular RNAs, due to their structural stability, have been used as biomarkers for a variety of diseases, including MC. In this study, circACSL1 exhibited extremely high stability and integrity even in the presence of RNase R, actinomycin D treatment, similar to most other circRNAs. In addition, in CVB3-infected mice and HL-1 cells, the high expression of circACSL1 was accompanied not only by the upregulation of inflamma ory factors IL-1β, IL-6, and TNF-α, and the abnormally high expression of myocardial injury markers CKMB, cTnI, and BNP, but also by abnormal autophagy and apoptosis in cardiac tissue and cells. However, knockdown of circACSL 1 was able to improve these conditions. It suggests that circACSL 1 makes a potential marker for VMC, and it is expected to be a therapeutic target for the treatment of VMC.

Circular RNAs often act as molecular sponges for miRNAs to indirectly regulate gene expression.[27] In this study,

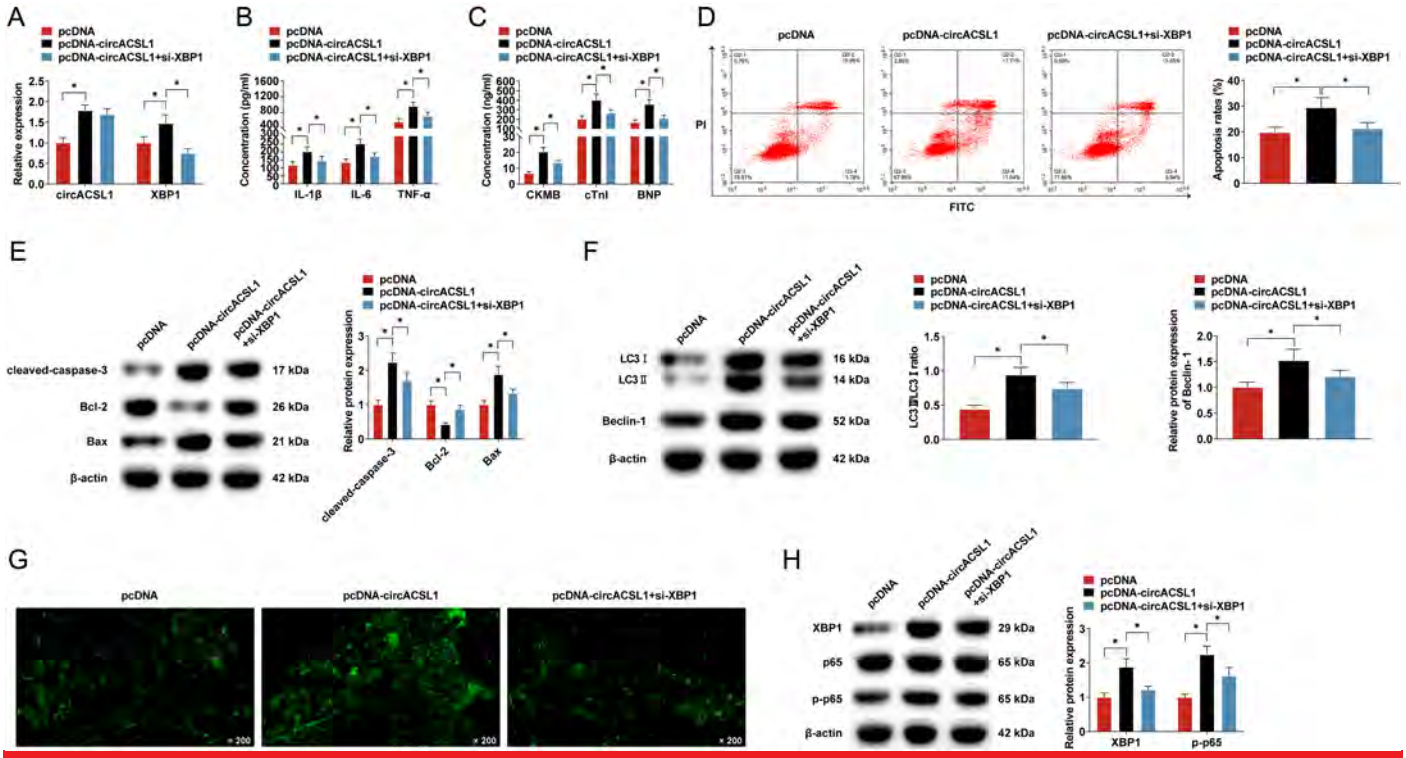

Figure 6. Depleting XBP1 saves the MC-promoting effect of overexpression of circ-ACSL1. (A) RT-qPCR detection of circ-ACSL1 and XBP1 in HL-1 cells; (B) ELISA determination of IL-1β, IL-6 and TNF-α in HL-1 cells; (C) ELISA determination of CK-MB, cTnI and BNP in HL-1 cell supernatant; (D) Flow cytometry detection of apoptotic rate of HL-1 cells; (E and F) Western blot analysis of apoptotic proteins in HL-1 cells; (G) MDC staining detection of autophagosomes; and (H) Western blot analysis of XBP1-related pathway protein. Detailed data in Supplementary Table 6. *$P < .05$.

circACSL 1 contains a conserved miR-7-5p target site, which was validated by luciferase reporter gene assay in the HL-1 in vitro cell model. A number of miRNAs have been reported to exhibit aberrant expression levels in VMC, and a growing body of evidence has highlighted the role of miRNAs in MC pathogenesis.[28-31] In agreement with these results, we found that miR-7-5p expression was downregulated in animal and cellular models of VMC, and knockdown of miR-7-5p expression reversed the ameliorative effects of knockdown of circACSL1 on myocardial tissues, cardiomyocyte inflamm - tion, myocardial injury, autophagy, and apoptosis. circACSL1 expression was negatively correlated with miR-7-5p expression in myocardial tissues and cells. These results suggest that circACSL 1 acts as a molecular sponge targeting miR-7-5p to fulfill its ole in VMC.

XBP1 expression is increased, and XIAP expression is decreased in LPS-induced H9c2 cells, and XBP1 aggravates LPS-induced cardiomyocyte injury by down-regulating XIAP through activating the NFκB signaling pathway.[32] Similar to this result, in our study, XBP1 was found to be highly expressed in CVB3-infected myocardial tissues and cardiomyocytes, and XBP1 was considered as a target gene of miR-7-5p, which showed a negative regulatory relationship with miR-7-5p expression. In addition, it can be positively regulated by circACSL1. Knockdown of XBP 1 was able to rescue the promotion of myocardial inflammation, apoptosis, and autophagy by overexpression of circACSL1.

In conclusion, the present study identified that circACSL1 was signifi antly upregulated in VMC and signifi antly exacerbated inflammation in VMC, resulting in increased apoptotic cell death and increased cellular autophagy. The mechanism by which this occurs may be that circACSL1 regulates XBP1 expression through targeting adsorption of miR-7-5p.

Availability of data and materials: The data that support the fin - ings of this study are available from the corresponding author, upon reasonable request.

Ethics Committee Approval: All animal experiments were complied with the ARRIVE guidelines and performed in accordance with the National Institutes of Health Guide for the Care and Use of Laboratory Animals. The experiments were approved by the Institutional Animal Care and Use Committee of Qinghai Province Cardio Cerebrovascular Disease Specialist Hospital (Approval no. 201911QH162; Approval date: November 16, 2019).

Peer-review: Externally peer-reviewed.

Author Contributions: Conceptualization – F.L., Y.T.; Methodology – X.Z., X.M.; Formal analysis – F.L.; Investigation – Y.T.; Data Curation – X.Z.; Original Draft Preparation – F.L., Y.T.; Writing—Review and Editing – X.M.; Project Administration – X.M. All authors have read and agreed to the published version of the manuscript.

Declaration of Interests: The authors have no conflicts of interest to declare.

Funding: The authors declare that this study received no financial support.

REFERENCES

1. Daba TM, Zhao Y, Pan Z. Advancement of mechanisms of Coxsackie virus B3-induced myocarditis pathogenesis and the potential therapeutic targets. *Curr Drug Targets*. 2019;20(14):1461-1473. [CrossRef]
2. Fung G, Luo H, Qiu Y, Yang D, McManus B. Myocarditis. *Circ Res*. 2016;118(3):496-514. [CrossRef]
3. Garmaroudi FS, Marchant D, Hendry R, et al. Coxsackievirus B3 replication and pathogenesis. *Future Microbiol*. 2015;10(4):629-653. [CrossRef]
4. Liu YL, Wu W, Xue Y, et al. MicroRNA-21 and -146b are involved in the pathogenesis of murine viral myocarditis by regulating TH-17 differentiation. *Arch Virol*. 2013;158(9):1953-1963. [CrossRef]
5. Wang X, Dai Y, Ding Z, Khaidakov M, Mercanti F, Mehta JL. Regulation of autophagy and apoptosis in response to angiotensin II in HL-1 cardiomyocytes. *Biochem Biophys Res Commun*. 2013;440(4):696-700. [CrossRef]
6. Yoshida GJ. Therapeutic strategies of drug repositioning targeting autophagy to induce cancer cell death: from pathophysiology to treatment. *J Hematol Oncol*. 2017;10(1):67. [CrossRef]
7. Meng Y, Sun T, Wu C, Dong C, Xiong S. Calpain regulates CVB3 induced viral myocarditis by promoting autophagic flux upon infection. *Microbes Infect*. 2020;22(1):46-54. [CrossRef]
8. Wang X, Guo Z, Ding Z, Mehta JL. Inflammation, autophagy, and apoptosis after myocardial infarction. *J Am Heart Assoc*. 2018;7(9). [CrossRef]
9. Zhang HD, Jiang LH, Sun DW, Hou JC, Ji ZL. CircRNA: a novel type of biomarker for cancer. *Breast Cancer*. 2018;25(1):1-7. [CrossRef]
10. Kristensen LS, Andersen MS, Stagsted LVW, Ebbesen KK, Hansen TB, Kjems J. The biogenesis, biology and characterization of circular RNAs. *Nat Rev Genet*. 2019;20(11):675-691. [CrossRef]
11. Wilusz JE, Sharp PA. Molecular biology. a circuitous route to noncoding RNA. *Science*. 2013;340(6131):440-441. [CrossRef]
12. Zhang L, Han B, Liu H, et al. Circular RNA circACSL1 aggravated myocardial inflammation and myocardial injury by sponging miR-8055 and regulating MAPK14 expression. *Cell Death Dis*. 2021;12(5):487. [CrossRef]
13. Zhang L, Han B, Wang J, et al. Differential expression profiles and functional analysis of circular RNAs in children with fulminant myocarditis. *Epigenomics*. 2019;11(10):1129-1141. [CrossRef]
14. Jin X, Feng CY, Xiang Z, Chen YP, Li YM. CircRNA expression pattern and circRNA-miRNA-mRNA network in the pathogenesis of nonalcoholic steatohepatitis. *Oncotarget*. 2016;7(41):66455-66467. [CrossRef]
15. Rong D, Sun H, Li Z, et al. An emerging function of circRNA-miRNAs-mRNA axis in human diseases. *Oncotarget*. 2017;8(42):73271-73281. [CrossRef]
16. Yuan W, Zhou R, Wang J, et al. Circular RNA Cdr1as sensitizes bladder cancer to cisplatin by upregulating APAF1 expression through miR-1270 inhibition. *Mol Oncol*. 2019;13(7):1559-1576. [CrossRef]
17. Zhou J, Li L, Hu H, et al. Circ-HIPK2 accelerates cell apoptosis and autophagy in myocardial oxidative injury by sponging miR-485-5p and targeting ATG101. *J Cardiovasc Pharmacol*. 2020;76(4):427-436. [CrossRef]
18. Zhu M, Li Y, Liu L, Zhai X. Circ_0057452 sponges miR-7-5p to promote keloid progression through upregulating GAB1. *Cell Cycle*. 2022;21(23):2471-2483. [CrossRef]
19. Ren XP, Wu J, Wang X, et al. MicroRNA-320 is involved in the regulation of cardiac ischemia/reperfusion injury by targeting heat-shock protein 20. *Circulation*. 2009;119(17):2357-2366. [CrossRef]
20. Li B, Li R, Zhang C, et al. MicroRNA-7a/b protects against cardiac myocyte injury in ischemia/reperfusion by targeting poly(ADP-ribose) polymerase. *PLoS One*. 2014;9(3):e90096. [CrossRef]
21. Gupta S, Deepti A, Deegan S, Lisbona F, Hetz C, Samali A. HSP72 protects cells from ER stress-induced apoptosis via enhancement of IRE1alpha-XBP1 signaling through a physical interaction. *PLoS Biol*. 2010;8(7):e1000410. [CrossRef]
22. Xu W, Wang C, Hua J. X-box binding protein 1 (XBP1) function in diseases. *Cell Biol Int*. 2021;45(4):731-739. [CrossRef]
23. Li B, Xie X. A20 (TNFAIP3) alleviates viral myocarditis through ADAR1/miR-1a-3p-dependent regulation. *BMC Cardiovasc Disord*. 2022;22(1):10. [CrossRef]
24. Altesha MA, Ni T, Khan A, Liu K, Zheng X. Circular RNA in cardiovascular disease. *J Cell Physiol*. 2019;234(5):5588-5600. [CrossRef]
25. Fan X, Weng X, Zhao Y, Chen W, Gan T, Xu D. Circular RNAs in cardiovascular disease: an overview. *BioMed Res Int*. 2017;2017:5135781. [CrossRef]
26. Fan S, Hu K, Zhang D, Liu F. Interference of circRNA HIPK3 alleviates cardiac dysfunction in lipopolysaccharide-induced mice models and apoptosis in H9C2 cardiomyocytes. *Ann Transl Med*. 2020;8(18):1147. [CrossRef]
27. Tay Y, Rinn J, Pandolfi PP. The multilayered complexity of ceRNA crosstalk and competition. *Nature*. 2014;505(7483):344-352. [CrossRef]
28. Corsten MF, Heggermont W, Papageorgiou AP, et al. The microRNA-221/-222 cluster balances the antiviral and inflamma ory response in viral myocarditis. *Eur Heart J*. 2015;36(42):2909-2919. [CrossRef]
29. Wang J, Han B. Dysregulated CD4+ T cells and microRNAs in myocarditis. *Front Immunol*. 2020;11:539. [CrossRef]
30. Goldberg L, Tirosh-Wagner T, Vardi A, et al. Circulating microRNAs: a potential biomarker for cardiac damage, inflamma ory response, and left ventricular function recovery in pediatric viral myocarditis. *J Cardiovasc Transl Res*. 2018;11(4):319-328. [CrossRef]
31. Deng B, Zheng X, Zheng X, Tian L, Zhang Y. Propofol inactivates NF-κB pathway to inhibit lipopolysaccharide-induced myocarditis via miR-142-5p/SOCS1 axis. *J Biol Regul Homeost Agents*. 2023;37(6):2927-2934.
32. Zhang C, Chen X, Wang C, Ran Y, Sheng K. Inhibition of XBP1 alleviates LPS-induced cardiomyocytes injury by upregulating XIAP through suppressing the NF-kappaB signaling pathway. *Inflammatio* . 2021;44(3):974-984. [CrossRef]

Supplementary Table 1. High Expression and Stability of Circ-ACSL1 in VMC

1. Animal experimental data

Indicators	Control (n = 6)	CVB3 (n = 6)	*P* value
IL-1β	13.2 ± 3.5	104.2 ± 19.6	< .0001
IL-6	21.3 ± 4.3	234.7 ± 48.8	< .0001
TNF-α	177.6 ± 40.3	623.1 ± 91.2	< .0001
CK-MB	5.64 ± 0.6	20.7 ± 2.04	< .0001
cTnI	103.4 ± 15.8	233.4 ± 30.5	< .0001
BNP	76.3 ± 15.3	188.6 ± 30.8	< .0001
Cleaved-caspase-3/β-actin	1.0 ± 0.091	1.89 ± 0.24	< .0001
Bcl2/β-actin	1.0 ± 0.113	0.39 ± 0.08	< .0001
Bax/β-actin	1.0 ± 0.137	1.81 ± 0.35	.0004
TUNEL positive cells (%)	8.6 ± 1.2	38.6 ± 5.4	.0007
(LC3 Ⅱ/LC3 Ⅰ)/β-actin	0.72 ± 0.08	0.95 ± 0.115	.0467
Beclin-1/β-actin	1.0 ± 0.14	1.52 ± 0.22	.0173
circACSL1	1.0 ± 0.13	3.34 ± 0.28	< .0001

2. Cellular experimental data

Indicators	Blank (n = 3)	CVB3 (n = 3)	*P* value
IL-1β	23.3 ± 3.89	105.14 ± 21.8	< .0001
IL-6	15.3 ± 2.34	162.3 ± 27.8	< .0001
TNF-α	136.5 ± 26.2	546.3 ± 105.2	< .0001
CK-MB	2.43 ± 0.45	4.38 ± 0.8	.0212
cTnI	88.6 ± 23.14	190.4 ± 41.02	.0201
BNP	106.8 ± 29.23	230.4 ± 35.11	.0094
Apoptosis rates (%)	4.89 ± 0.61	22.05 ± 2.81	.0005
Cleaved-caspase-3/β-actin	1.0 ± 0.13	1.81 ± 0.28	.0105
Bcl2/β-actin	1.0 ± 0.12	0.63 ± 0.093	.0135
Bax/β-actin	1.0 ± 0.09	2.53 ± 0.33	.0015
(LC3 Ⅱ/LC3 Ⅰ)/β-actin	0.22 ± 0.03	0.94 ± 0.11	.0004
Beclin-1/β-actin	1.0 ± 0.15	2.78 ± 0.23	.0004
circACSL1	1.0 ± 0.098	2.28 ± 0.15	.0002

3. RNase R

	MOCK (n = 3)	RNase R (n = 3)	*P* value
ACSL1	1.0 ± 0.12	0.47 ± 0.06	.0024
circACSL1	1.0 ± 0.14	1.14 ± 0.16	.3177

Supplementary Table 2. Knocking down circ-ACSL1 inhibits inflammation, apo tosis, and autophagy of VMC cardiomyocytes

1. Animal experimental data

Indicators	sh-NC (n = 6)	sh-circACSL1 (n = 6)	*P* value
circACSL1	1.0 ± 0.058	0.38 ± 0.127	< .0001
IL-1β	130.30 ± 26.2	53.2 ± 10.5	< .0001
IL-6	163.2 ± 33.2	75.6 ± 13.6	.0001
TNF-α	645.8 ± 123.8	403.4 ± 90.2	.0031
CK-MB	17.4 ± 2.8	8.47 ± 1.4	< .0001
cTnI	200.6 ± 33.8	105.4 ± 23.6	.0002
BNP	183.4 ± 31.5	68.5 ± 15.9	< .0001
TUNEL positive cells (%)	38.06 ± 5.52	21.2 ± 3.57	< .0001
Cleaved-caspase-3/β-actin	1.0 ± 0.091	0.702 ± 0.101	.003
Bcl2/β-actin	1.0 ± 0.103	1.83 ± 0.25	< .0001
Bax/β-actin	1.0 ± 0.127	0.71 ± 0.14	.0037
(LC3 Ⅱ/LC3 Ⅰ)/β-actin	0.88 ± 0.14	0.62 ± 0.07	.0451
Beclin-1/β-actin	1.0 ± 0.1	0.77 ± 0.09	.0415

2. Cellular experimental data

Indicators	si-NC (n = 3)	si-circACSL1 (n = 3)	*P* value
circACSL1	1.0 ± 0.133	0.33 ± 0.086	.0018
IL-1β	112.5 ± 21.6	33.6 ± 24.3	.0137
IL-6	143.2 ± 33.2	57.5 ± 9.4	.0126
TNF-α	558.7 ± 88.9	334.8 ± 59	.0221
CK-MB	5.68 ± 0.74	2.12 ± 0.38	.0018
cTnI	243.4 ± 41.7	138.6 ± 19.6	.0170
BNP	203.8 ± 35.2	96.4 ± 15.1	.0083
Apoptosis rates (%)	34.3 ± 5.2	15.6 ± 2.68	.0052
Cleaved-caspase-3/β-actin	1.0 ± 0.104	0.74 ± 0.076	.0250
Bcl2/β-actin	1.0 ± 0.12	1.66 ± 0.18	.0062
Bax/β-actin	1.0 ± 0.09	0.79 ± 0.095	.0498
(LC3 Ⅱ/LC3 Ⅰ)/β-actin	0.92 ± 0.12	0.35 ± 0.05	.0016
Beclin-1/ β -actin	1.0 ± 0.07	0.75 ± 0.1	.0239

Supplementary Table 3. Circ-ACSL1 Targets miR-7-5p Adsorption

1. Relative expression of miR-7-5p in mouse myocardial tissue

	Control (n = 6)	CVB3 (n = 6)	*P* value
miR-7-5p	1.0 ± 0.13	0.64 ± 0.08	.0002

2. Relative expression of miR-7-5p in cell

	Blank (n = 3)	CVB3 (n = 3)	*P* value
miR-7-5p	1.0 ± 0.12	0.72 ± 0.11	.0424

3. Relative luciferase activity

	WT-circACSL1 (n = 3)	Mut-circACSL1 (n = 3)	*P* value
mimic NC	1.0 ± 0.12	0.28 ± 0.039	.0006
miR-7-5p mimic	1.0 ± 0.10	0.954 ± 0.153	.6854

4. RNA pull down

	Bio-NC (n = 3)	Bio-miR-7-5p-Wt (n = 3)	Bio-miR-7-5p-Mut (n = 3)	P value (Bio-NC vs. Bio-miR-7-5p-Wt)	P value (Bio-miR-7-5p-Wt vs. Bio-miR-7-5p-Mut)
Relative enrichment of circACSL1	1.0 ± 0.186	14.47 ± 2.54	5.21 ± 1.24	< .05	< .05

5. Relative expression of miR-7-5p in mouse myocardial tissue

	sh-NC (n = 6)	sh-circACSL1 (n = 6)	*P* value
miR-7-5p	1.0 ± 0.12	2.60 ± 0.34	< .05

6. Relative expression of miR-7-5p in cell

	si-NC (n = 3)	si-circACSL1 (n = 3)	*P* value
miR-7-5p	1.00 ± 0.14	1.90 ± 0.29	.0084

Supplementary Table 4. miR-7-5p Downregulation can Reduce the Therapeutic Effect of Depleting Circ-ACSL1 on VMC

	si-NC (n = 3)	si-circACSL1+inhibitor (n = 3)	si-circACSL1+miR-7-5p inhibitor (n = 3)	*P* value (si-circACSL1+inhibitor vs. si-NC)	*P* value (si-circACSL1+miR-7-5p inhibitor vs. si-circACSL1+inhibitor)
circACSL1	1.0 ± 0.130	0.39 ± 0.08	0.36 ± 0.06	0.0023	.6367
miR-7-5p	1.0 ± 0.122	1.34 ± 0.20	0.53 ± 0.072	0.0313	.0027
IL-1β	112.5 ± 21.6	30.6 ± 24.3	89.3 ± 12.5	0.012	.0205
IL-6	143.2 ± 33.2	53.5 ± 9.4	125.8 ± 12.58	0.0108	.0013
TNF-α	558.7 ± 88.9	314.8 ± 58.5	468.33 ± 60.8	0.0165	.0345
CK-MB	5.68 ± 1.08	2.42 ± 0.38	13.4 ± 1.96	0.0079	.0007
cTnI	243.4 ± 41.7	128.6 ± 23.6	396.4 ± 68.6	0.0143	.0031
BNP	200.8 ± 35.2	106.4 ± 15.1	348.9 ± 49.2	0.0130	.0012
Apoptosis rates (%)	34.3 ± 5.2	14.76 ± 1.92	18.8 ± 4.2	0.0043	.0021
Cleaved-caspase-3/β-actin	1.0 ± 0.130	0.39 ± 0.055	0.77 ± 0.101	0.0017	.0046
Bcl2/β-actin	1.0 ± 0.104	1.62 ± 0.18	1.11 ± 0.11	0.0067	.0138
Bax/β-actin	1.0 ± 0.120	0.38 ± 0.1	1.89 ± 0.24	0.0023	.0005
(LC3Ⅱ/LC3Ⅰ)/β-actin	0.91 ± 0.11	0.32 ± 0.04	0.63 ± 0.07	0.009	.0026
Beclin-1/β-actin	1.0 ± 0.07	0.39 ± 0.05	0.79 ± 0.11	0.0002	.0044

Supplementary Table 5. miR-7-5p Targets XBP1

1. Relative mRNA expression of XBP1 in mouse myocardial tissue

	Control (n = 6)	CVB3 (n = 6)	*P* value
XBP1 mRNA	1.0 ± 0.15	4.26 ± 0.48	.0003

2. Relative mRNA expression of XBP1 in cell

	Blank (n = 3)	CVB3 (n = 3)	*P* value
XBP1 mRNA	1.0 ± 0.11	3.47 ± 0.58	.0019

3. Relative protein expression of XBP1 in mouse myocardial tissue

	Control (n = 6)	CVB3 (n = 6)	*P* value
XBP1	1.0 ± 0.14	1.53 ± 0.19	.0177

4. Relative protein expression of XBP1 in cell

	Blank (n = 3)	CVB3 (n = 3)	*P* value
XBP1	1.0 ± 0.1	2.51 ± 0.33	.0016

5. Relative luciferase activity

	1 mimic NC (n = 3)	miR-7-5p mimic (n = 3)	*P* value
WT-XBP	1.0 ± 0.11	0.63 ± 0.098	.0122
Mut-XBP1	1.0 ± 0.14	0.928 ± 0.124	.5414

6. RNA pull down

	Bio-NC (n = 3)	Bio-miR-7-5p-Wt (n = 3)	Bio-miR-7-5p-Mut (n = 3)	*P* value (Bio-NC vs. Bio-miR-7-5p-Wt)	*P* value (Bio-miR-7-5p-Wt vs. Bio-miR-7-5p-Mut)
Relative enrichment of XBP1	1.0 ± 0.158	12.26 ± 2.54	6.37 ± 1.24	.0016	.0226

7. Relative mRNA expression of XBP1

	mimic-NC (n = 3)	miR-7-5p-mimic (n = 3)	*P* value	inhibitor-NC (n = 3)	miR-7-5p inhibitor (n = 3)	*P* value
XBP1 mRNA	1.0 ± 0.133	0.54 ± 0.084	.0072	1.0 ± 0.10	3.20 ± 0.52	.0020

8. Relative protein expression of XBP1

	mimic-NC (n = 3)	miR-7-5p-mimic (n = 3)	*P* value	inhibitor-NC (n = 3)	miR-7-5p inhibitor (n = 3)	*P* value
XBP1	1.0 ± 0.11	0.37 ± 0.05	.0009	1.0 ± 0.13	1.6 ± 0.19	.0110

Supplementary Table 6. Circ-ACSL1 Overexpression Promotes VMC, But this Effect is Saved by Depleting XBP1

	pcDNA (n = 3)	pcDNA-circACSL1 (n = 3)	pcDNA-circACSL1+si-XBP1 (n = 3)	*P* value (pcDNA-circACSL1 vs. pcDNA)	*P* value (pcDNA-circACSL1+si-XBP1 vs. pcDNA-circACSL1)
circACSL1	1.0 ± 0.125	1.78 ± 0.14	1.69 ± 0.14	.0020	.4751
XBP1	1.0 ± 0.147	1.47 ± 0.21	0.746 ± 0.112	.0337	.0062
IL-1β	116.7 ± 21.6	201.8 ± 32.1	132.3 ± 23.8	.0189	.0395
IL-6	134.3 ± 21.3	252.3 ± 30.4	171.2 ± 22.3	.0053	.0204
TNF-α	564.2 ± 87.1	958.2 ± 103.6	707.7 ± 101.7	.0073	.0404
CK-MB	6.74 ± 1.1	20.3 ± 2.8	13.5 ± 1.3	.0015	.0189
cTnI	201.8 ± 33.4	400.3 ± 64.9	263.5 ± 36.4	.0092	.0034
BNP	167.5 ± 25.9	357.3 ± 48.4	210.1 ± 33.7	.0039	.0124
Apoptosis rates (%)	19.7 ± 2.1	29.4 ± 3.9	21.2 ± 2.4	.0192	.0362
Cleaved-caspase-3/β-actin	1.0 ± 0.13	2.23 ± 0.28	1.69 ± 0.25	.0023	.0412
Bcl2/β-actin	1.0 ± 0.11	0.42 ± 0.055	0.86 ± 0.12	.0012	.0045
Bax/β-actin	1.0 ± 0.12	1.88 ± 0.24	1.33 ± 0.12	.0047	.0238
(LC3 Ⅱ/LC3 Ⅰ)/β-actin	0.44 ± 0.06	0.94 ± 0.11	0.74 ± 0.09	.0022	.0378
Beclin-1/β-actin	1.0 ± 0.104	1.62 ± 0.22	1.21 ± 0.12	.0116	.0472
XBP1	1.0 ± 0.127	1.88 ± 0.24	1.21 ± 0.11	.0049	.0117
p-p65	1.0 ± 0.09	2.24 ± 0.25	1.62 ± 0.25	.0013	.0385